Analytic confirmation that the factorized formula for harmonic generation involves the exact photorecombination cross section

M. V. Frolov, N. L. Manakov, and T. S. Sarantseva
Department of Physics, Voronezh State University, 394006 Voronezh, Russia

Anthony F. Starace
Department of Physics and Astronomy, The University of Nebraska, Lincoln Nebraska 68588-0299, USA
(Received 13 February 2011; published 26 April 2011)

High-order-harmonic generation (HHG) by atoms in a strong laser field is analyzed theoretically, taking into account atomic potential effects beyond the strong field approximation (SFA). Our analytical derivation extends the time-dependent effective range (TDER) theory, developed previously for a short-range potential supporting only a single bound state, to the case of a potential supporting two bound states having different angular momenta and dynamically interacting with the continuum. In contrast to the SFA and the single-state TDER model, in both of which the HHG rates in the region of the high-energy plateau cutoff involve only the plane-wave (first Born) approximation for the photorecombination cross section, our analytic expression for the HHG rates in the two-state TDER model involves the exact photorecombination cross section for this model. These results justify the factorization of HHG rates in the high-energy plateau region in terms of the electron wave packet and the *exact* (non-Born) photorecombination cross section, which was suggested previously using only phenomenological arguments.

DOI: 10.1103/PhysRevA.83.043416 PACS number(s): 32.80.Rm, 42.65.Ky, 32.80.Wr

I. INTRODUCTION

High-order-harmonic generation (HHG) is nowadays the main focus of intense laser-atom physics owing to its significant potential impact in both technological and scientific applications. First, it may allow the production of table-top sources of intense coherent radiation with wavelengths important for different applications, such as those in the "water window" [1–4]. Second, HHG is the primary means for producing ultrashort, attosecond pulses, which play a central role in attosecond science [5,6]. Finally, it has become increasingly apparent recently that this process demonstrates a high potential for extracting structural information on target atoms or molecules. The idea of using HHG to image atomic and molecular structures was formulated first in Ref. [7] (see also Ref. [8]), where the semiclassical three-step scenario for the HHG process [9,10] was utilized to extract the Fourier transform of an atomic wave function. A significant advance suggested by Lin and coworkers [11–13], based upon numerical solutions of the time-dependent Schrödinger equation (TDSE), was the following phenomenological parametrization for HHG rates ($\mathcal{R}_N$) in the high-energy part of the HHG spectrum

$$\mathcal{R}_N = W(E)\sigma_{\rm rec}(E), \quad E = \hbar\Omega - |E_0|. \tag{1}$$

In Eq. (1) $|E_0|$ is the atomic binding energy, Ω is the frequency of the Nth harmonic, $\sigma_{\rm rec}(E)$ is the *exact* (atom-specific) photorecombination cross section of the active electron with its parent ion (forming the atom from whose valence subshell it was ionized by the pump laser field), and $W(E)$ is the so-called "electronic wave packet" (EWP). In Refs. [11–13] the EWP is a fitted parameter. Both numerical simulations and experimental data show that its shape is essentially independent of the atom used to generate the HHG spectrum. An explicit form of the EWP (in terms of an Airy function) was obtained analytically in Ref. [14] (cf. also Ref. [15]) within the framework of the quasistationary quasienergy state (QQES) approach (cf., e.g., Ref. [16]) applied to a model system. The analytic expression for the EWP showed that its dependence on the particular atom stems only from two parameters of the active electron's initial bound state $\psi_0(\mathbf{r})$ [i.e., $|E_0|$ and the asymptotic coefficient in $\psi_0(\mathbf{r})$ at large r]. The model system for which the derivation [14] was carried out is that of a single electron bound in a short-range potential $U(r)$ that interacts with a strong monochromatic laser field (i.e., the time-dependent effective range (TDER) model [17,18]). The generalization to neutral atoms of the analytic formula for HHG rates obtained for the TDER model system was presented in Ref. [15].

The validity of the parametrization (1) has been confirmed recently by a number of experiments. First, experiments on the HHG spectrum of Ar [19,20] observed signatures of the Cooper minimum in the photoionization cross section of Ar. (The photoionization cross section is proportional to the photorecombination cross section according to the principle of detailed balance.) Second, based on the parametrization (1), both enhancement and suppression of individual harmonics observed in experiments on the HHG spectra of laser-produced plasmas of singly charged ions of the transition metals Cr and Mn [21,22] were explained in Ref. [23] as originating from "giant dipole" resonance features in the photoionization cross sections of Cr^+ and Mn^+ ions. Third, Ref. [15] predicted a broad resonance-like feature in the HHG spectrum of the $5p$-subshell of Xe (originating from the well-known giant dipole resonance in the $4d$-subshell photoionization cross section of Xe); this prediction has now been confirmed experimentally [24]. Despite the fact that both the aforementioned experiments and the numerical solutions of the TDSE [11–13] show that the parametrization (1) seems to be quite reliable, at the present time there does not yet exist any formal theoretical justification of Eq. (1) based on an accurate quantum-mechanical derivation involving the exact

 ©2011 American Physical Society

photorecombination cross section (as opposed to the plane-wave approximation to the photorecombination cross section, as in the derivation of Eq. (1) in Ref. [14]). Given the practical importance of the parametrization in Eq. (1), such a quantum-mechanical derivation, even for a simplified model of the atom, is important not only for justifying this parametrization but also for providing an accurate understanding of the physics of the HHG process.

Although the TDER theory has allowed us to obtain an analytic form of the EWP $W(E)$ [14], this theory, in common with the strong field approximation (SFA) description of the HHG process [25], yields the plane-wave (first Born approximation) result for $\sigma_{\rm rec}(E)$ in Eq. (1). Within the SFA, this shortcoming is due to the neglect of any interaction between the active atomic electron in the laser-dressed continuum and the atomic potential, while within the TDER model, in which the atomic potential has only a single bound state [17], this shortcoming has a different origin. In the single-state TDER (SS TDER) theory only the l-wave phase shift $\delta_l(E)$, for an electron scattering from the potential $U(r)$ is nonzero, where l corresponds to the angular momentum of the single bound state in the potential $U(r)$. However, according to electric dipole selection rules for the photoionization process, it is the scattering phase shifts $\delta_{l\pm1}(E)$ that contribute primarily to $\sigma_{\rm rec}(E)$. In the SS TDER theory these phases are unaffected by the potential $U(r)$. That is why our derivations in Ref. [14] for the SS TDER model result in the parametrization (1) in which $\sigma_{\rm rec}(E)$ is represented by its plane-wave approximation.

In this paper we generalize the SS TDER theory to the case of two (s and p) bound states in the potential $U(r)$ and show that within this more general two-state TDER (TS TDER) model the HHG rates can indeed be presented in the form (1) with the exact (non-Born) result for $\sigma_{\rm rec}(E)$. In addition our derivations show that an analytic form of the EWP $W(E)$ in the TS TDER theory remains the same as in the SS TDER model, thereby providing further theoretical support for the weak sensitivity of the EWP $W(E)$ in Eq. (1) to the details of the atomic structure.

The paper is organized as follows. In Sec. II we describe the TS TDER model. Specifically, in Sec. II A we focus on the two-state effective range theory model in the absence of the laser field. In Sec. II B the laser field is introduced and exact equations for the complex quasienergy and QQES (or Floquet) wave functions in the TS TDER theory are derived. In Sec. II C two levels of approximation for the QQES wave functions are made that are valid in the low-frequency tunneling limit. In Sec. III we apply these results to the description of HHG, derive a factorized analytic result for the HHG amplitude (and the corresponding HHG rates) in the tunneling limit, and show that these results are in perfect agreement with exact numerical TS TDER results in the high-energy part of the HHG spectrum. In Sec. IV we discuss our results and present some conclusions.

II. TDER THEORY FOR A SHORT-RANGE POTENTIAL HAVING TWO BOUND STATES

A. Field-free two-state model

We consider an electron in a three-dimensional short-range potential $U(r)$ [where $U(r)=0$ for $r>r_c$] having two bound states, with angular momenta $l=0$ and 1, respectively. Our basic assumption is that in elastic electron scattering from the potential $U(r)$ only two scattering phases $\delta_l(k)$ are nonzero: the s-wave and p-wave phases, $\delta_0(k)$ and $\delta_1(k)$, where $k=\sqrt{2mE}/\hbar$. According to effective range theory for low-energy electron scattering [26], we parametrize these phases in terms of the scattering length a_l and the effective range r_l, which are parameters of the problem

$$k^{2l+1}\cot\delta_l(k) = -1/a_l + r_l k^2/2. \tag{2}$$

Since the electron is free outside the potential well $U(r)$, its scattering wave function $\psi^{(+)}_{\mathbf{k}}(\mathbf{r})$, for $r>r_c$ may be written in terms of the parametrization (2) as follows:

$$\begin{aligned}\psi^{(+)}_{\mathbf{k}}(\mathbf{r}) &= e^{i\mathbf{k}\cdot\mathbf{r}} + \frac{1}{2}(e^{2i\delta_0}-1)h^{(1)}_0(kr)\\ &\quad+\frac{3i}{2}(e^{2i\delta_1}-1)h^{(1)}_1(kr)\cos\theta = e^{i\mathbf{k}\cdot\mathbf{r}}\\ &\quad+i\frac{k}{\mathcal{R}_0(E)}h^{(1)}_0(kr) - \frac{3k^3}{\mathcal{R}_1(E)}h^{(1)}_1(kr)\cos\theta,\end{aligned} \tag{3}$$

where $\cos\theta=\hat{\mathbf{k}}\cdot\hat{\mathbf{r}}$, $h^{(1)}_l(kr)$ is the spherical Hankel function of the first kind, and

$$\mathcal{R}_l(E) = -a_l^{-1} + r_l k^2/2 - ik^{2l+1}. \tag{4}$$

The physical meaning of the factor $\mathcal{R}_l(E)$ (which enters also into key equations of the TDER theory) follows from Eq. (3): it determines the partial wave amplitudes $f_l(E)$, for elastic electron scattering from the potential $U(r)$ in the s-wave and p-wave channels

$$f_l(E) \equiv (e^{2i\delta_\ell}-1)/2ik = k^{2l}/\mathcal{R}_l(E). \tag{5}$$

Assuming that both scattering lengths a_0 and a_1 are positive, the potential $U(r)$ supports two bound states dynamically interacting with the continuum through the scattering phases $\delta_0(k)$ and $\delta_1(k)$. The wave functions $\psi_0(\mathbf{r})$ and $\psi_1(\mathbf{r})$ and energies E_0 and E_1 of these bound states can be obtained as the residues of the continuum state (3) at the negative energy poles $E=E_l$ ($l=0,1$) given by the equation $\mathcal{R}_l(E_l)=0$. Their expressions are

$$E_0 = -\frac{\hbar^2\kappa_0^2}{2m},\quad \psi_0(\mathbf{r}) = -\kappa_0^{3/2}C_{\kappa_0}h^{(1)}_0(i\kappa_0 r)Y_{00}(\hat{\mathbf{r}}), \tag{6}$$

$$E_1 = -\frac{\hbar^2\kappa_1^2}{2m},\quad \psi_1(\mathbf{r}) = -i\kappa_1^{3/2}C_{\kappa_1}h^{(1)}_1(i\kappa_1 r)Y_{1m}(\hat{\mathbf{r}}), \tag{7}$$

where the parameters κ_l and C_{κ_l} can be expressed in terms of a_l and r_l

$$\begin{aligned}a_l^{-1} &= (-1)^l\kappa_l^{2l+1} - r_l\kappa_l^2/2,\\ 2C_{\kappa_l}^{-2} &= (-1)^l(2l+1) - r_l\kappa_l^{1-2l},\end{aligned} \tag{8}$$

in agreement with general relations of the effective range theory [27,28]. For $\kappa_l r \gg 1$, the wave functions (6) and (7) have the standard form for a finite-range potential

$$\psi_l(\mathbf{r})|_{\kappa_l r\gg1} = C_{\kappa_l}\sqrt{\kappa_l}r^{-1}\exp(-\kappa_l r)Y_{lm}(\hat{\mathbf{r}}),$$

where C_{κ_l} is the (dimensionless) asymptotic coefficient.

Using the wave functions (3), (6), and (7), the differential photorecombination cross section for an electron with wave

vector $\mathbf{k}$ ($k = \sqrt{2mE}/\hbar$) that emits a linearly polarized photon with frequency $\Omega = (E - E_l)/\hbar$ (and polarization vector $\mathbf{e}_z$ directed along the vector $\mathbf{k}$) when it recombines into the bound state $\psi_l(\mathbf{r})$ is

$$\sigma_{\rm rec}^{(l)}(E) \equiv \frac{d^2\sigma_{\rm rec}^{(l)}(E)}{d\Omega_{\hat{\mathbf{k}}} d\Omega_{\mathbf{e}_z}} = \frac{\Omega^3}{2\pi c^3}\frac{1}{a_B k}\left|f_{\rm rec}^{(l)}(k)\right|^2, \tag{9}$$

where a_B is the Bohr radius and

$$f_{\rm rec}^{(l)}(k) = \langle \psi_{\mathbf{k}}^{(+)}(\mathbf{r})|z|\psi_l(\mathbf{r})\rangle. \tag{10}$$

Though wave functions (3), (6), and (7) are valid for $r > r_c$ and diverge $\sim r^{-l-1}$ as $r \to 0$, the dipole matrix element (10) with these wave functions is finite, so that the amplitudes $f_{\rm rec}^{(l)}(k)$ for recombination to the ground ($l = 0$) and excited ($l = 1, m = 0$) states are

$$f_{\rm rec}^{(0)}(k) = iC_{\kappa_0}\frac{4\sqrt{\pi\kappa_0}k}{(k^2+\kappa_0^2)^2}\left[1 + \frac{(\kappa_0 - 2ik)(\kappa_0 + ik)^2}{2\mathcal{R}_1(E)}\right], \tag{11}$$

$$f_{\rm rec}^{(1)}(k) = -C_{\kappa_1}\frac{2\sqrt{3\pi}}{\sqrt{\kappa_1}(k^2+\kappa_1^2)^2} \times\left[k^2 - \kappa_1^2 - \frac{(2\kappa_1 - ik)(\kappa_1 + ik)^2}{3\mathcal{R}_0(E)}\right]. \tag{12}$$

Owing to electric dipole selection rules, the expressions for $f_{\rm rec}^{(0)}(k)$ or $f_{\rm rec}^{(1)}(k)$ involve only the phase shifts for p-wave or s-wave scattering, respectively. Therefore, the cross sections $\sigma_{\rm rec}^{(l)}(E)$ for the single-bound-state model coincide with those using the plane-wave approximation for the scattering state (3), that is, neglecting terms involving $\mathcal{R}_l^{-1}(E)$ in Eqs. (11) and (12). [Note that, for a negative scattering length a_1, the potential $U(r)$ supports only a single bound s-state $\psi_0(\mathbf{r})$, for which, however, the amplitude $f_{\rm rec}^{(0)}(k)$ still has the same form (11).]

Our aim in this paper is to show that by treating the nonperturbative interactions of an electron with both a potential $U(r)$ and an intense laser field within the TS TDER model we are able to derive the factorized result (1) for HHG rates in which the photorecombination amplitudes are given by the exact results, Eqs. (11) or (12), within this two-state model.

B. Exact equations for the complex quasienergy and QQES wave functions in the TS TDER model

Under the action of a linearly polarized, monochromatic field with electric vector $\mathbf{F}(t) = \mathbf{F}\cos\omega t$, the wave function for an electron bound initially either in the $\psi_0(\mathbf{r})$ or $\psi_1(\mathbf{r})$ state evolves to the field-dressed QQES wave function $\Phi_\epsilon(\mathbf{r},t)$ [$\Phi_\epsilon(t) = \Phi_\epsilon(t+T), T = 2\pi/\omega$] having complex quasienergy ϵ (with $\epsilon \to E_0$ or E_1 as $F \to 0$). The advantage of the TDER approach is that it avoids the solution of the four-dimensional (in $\mathbf{r}$ and t) Schrödinger eigenvalue equation for $\Phi_\epsilon(\mathbf{r},t)$ and ϵ (cf. Ref. [16]) by reducing the problem to the solution of an infinite system of linear homogeneous equations [17]. The key idea of this approach [formulated first in Ref. [29] for a weakly bound electron subjected to a long-range static perturbation $V(\mathbf{r})$] is that the interactions of the electron with the field $\mathbf{F}(t)$ (in the electric dipole approximation)

$$V(\mathbf{r},t) = -e\mathbf{r}\cdot\mathbf{F}(t), \tag{13}$$

and with the short-range potential $U(r)$ (with small radius r_c) are significant in essentially nonoverlapping spatial domains: $V(\mathbf{r},t)$ is most significant for $r > r_c$, while $U(r)$ is significant only for $r \lesssim r_c$. Moreover, the action of the potential $U(r)$ can be replaced by the appropriate boundary condition for the QQES wave function $\Phi_\epsilon(\mathbf{r},t)$ formulated at $r_c \lesssim r \ll \kappa_l^{-1}$, while outside the potential well $U(r)$ the function $\Phi_\epsilon(\mathbf{r},t)$ can be constructed from the solutions of the Schrödinger equation for a free electron in the field $\mathbf{F}(t)$. For a bound electron in a potential $U(r)$ supporting two bound states, the effective range theory for description of its interaction with a static electric field $\mathbf{F}$ has been utilized in Ref. [28]. Here we treat the case of a time-dependent electric field in a way similar to our development of the SS TDER theory [17].

The wave function $\Phi_\epsilon(\mathbf{r},t)$ for $r > r_c$ [where $U(r) = 0$] in the case of a potential $U(r)$ having two bound states with angular momenta $l = 0$ and 1 can be presented as the sum of two terms involving the retarded Green function, $G(\mathbf{r},t;\mathbf{r}',t')$, for a free electron in the field $\mathbf{F}(t)$ and its spatial derivatives

$$\Phi_\epsilon(\mathbf{r},t) = \mathcal{N}\sum_{l=0}^{1}\mathcal{D}_{l,m}(\mathbf{r}')\chi_\epsilon^{(l,m)}(\mathbf{r},\mathbf{r}',t)|_{r'=0}, \tag{14}$$

$$\chi_\epsilon^{(l,m)}(\mathbf{r},\mathbf{r}',t) = \int_{-\infty}^{t} dt' e^{i\epsilon(t-t')/\hbar} f^{(l,m)}(t')G(\mathbf{r},t;\mathbf{r}',t'), \tag{15}$$

where $\mathcal{N}$ is a normalization factor. (Details on the normalization of QQES wave functions can be found in Ref. [30].) The differential operator $\mathcal{D}_{l,m}(\mathbf{r})$ has the following form:

$$\begin{aligned}\mathcal{D}_{0,m}(\mathbf{r}) &= \delta_{m,0}, \quad \mathcal{D}_{1,0}(\mathbf{r}) = \sqrt{3}\kappa_1^{-1}\partial/\partial z,\\ \mathcal{D}_{1,\pm1}(\mathbf{r}) &= \sqrt{3/2}\kappa_1^{-1}(\partial/\partial x \pm i\partial/\partial y).\end{aligned} \tag{16}$$

[Note that Eq. (14) corresponds to the QQES $\Phi_\epsilon(\mathbf{r},t)$ with a given angular momentum projection m, which is a conserved quantum number for the case of a linearly polarized field $\mathbf{F}(t)$; its value is given by that of the initial bound state, $\psi_0(\mathbf{r})$ or $\psi_1(\mathbf{r})$.] The functions $f^{(0,0)}(t)$ and $f^{(1,m)}(t)$ in Eq. (15) are periodic functions of time that satisfy equations obtained using the prescribed boundary conditions for $\Phi_\epsilon(\mathbf{r},t)$ at small r ($r_c \lesssim r \ll \kappa_l^{-1}$) for the case of a short-range potential $U(r)$. These conditions are similar to those for the SS TDER theory [17]

$$\int \Phi_\epsilon(\mathbf{r},t)Y_{lm}^*(\hat{\mathbf{r}})d\Omega_{\mathbf{r}} \sim \sum_s [r^{-l-1} + \cdots + B_l(\epsilon + s\hbar\omega)(r^l + \cdots)]f_s^{(l,m)}e^{-is\omega t}, \tag{17}$$

where $f_s^{(l,m)}$ are the Fourier coefficients of $f^{(l,m)}(t)$, while the term $B_l(E)$ is proportional to $k^{2l+1}\cot\delta_l(k)$, so that it can be parameterized similarly to Eq. (2)

$$(2l+1)!!(2l-1)!!B_l(E) = -1/a_l + r_l k^2/2. \tag{18}$$

Calculating the s-wave and p-wave components of the QQES wave function (14) [using the Feynman form of $G(\mathbf{r},t;\mathbf{r}',t')$ in terms of the classical action], and then matching their small-r expansions to the boundary condition (17) for $l = 0$ and 1, we obtain a coupled system of two homogeneous integrodifferential equations, which together represent the eigenvalue problem for the functions $f^{(0,0)}(t)$ and $f^{(1,m)}(t)$

and the quasienergy ϵ. As in the SS TDER model [17], instead of solving these latter equations it is more convenient to solve the equivalent system of linear homogeneous equations for the Fourier coefficients $f_s^{(l,m)}$ of $f^{(l,m)}(t)$. The final results differ for the cases $|m| = 1$ [corresponding to initially populated p states $\psi_1(\mathbf{r})$ with $m = \pm 1$] and $m = 0$. In the latter case, the results depend on the initial bound state [$\psi_0(\mathbf{r})$ or $\psi_1(\mathbf{r})$ with $m = 0$].

For the QQESs with $m = \pm 1$, the term with $l = 0$ does not contribute to the right-hand side on Eq. (14) (since the states ψ_0 and $\psi_{1,m=\pm 1}$ are not mixed by a linearly polarized field due to electric dipole selection rules). Thus the matrix equation for ϵ and the Fourier coefficients of $f^{(1,m=\pm 1)}(t)$ coincides with that for the single ($\psi_{1,m=\pm 1}$)-state TDER model [17]

$$\sum_{s'} \left[\bar{M}_{s,s'}^{(pp)}(\epsilon) - \mathcal{R}_1(\epsilon)\delta_{ss'}\right] f_{s'}^{(1,\pm 1)} = 0, \tag{19}$$

where $\mathcal{R}_1(\epsilon)$ is given by Eq. (4). Since only "even" coefficients $f_{s=2k}^{(1,\pm 1)}$ enter Eq. (19) [17], we define $\bar{M}_{k,k'}^{(pp)} \equiv \bar{M}_{s=2k,s'=2k'}^{(pp)}$, where the explicit form of $\bar{M}_{k,k'}^{(pp)}$ in terms of integrals of Bessel functions $J_n(x)$ is given by Eq. (A1).

A close inspection of the coupled integrodifferential equations for $f^{(0,0)}(t) \equiv f^{(0)}(t)$ and $f^{(1,m=0)}(t) \equiv f^{(1)}(t)$ shows that, for the case of an initial s-state $\psi_0(\mathbf{r})$, the function $f^{(0)}(t)$ involves only even Fourier coefficients $f_{s=2k}^{(0)} \equiv f_k^{(0)}$ (which are normalized by the condition $f_0^{(0)} = 1$), while the Fourier coefficients of $f^{(1)}(t)$ are odd, $f_{s=2k+1}^{(1)} \equiv f_k^{(1)}$. Using these notations, the system of coupled linear homogeneous equations for $f_k^{(0)}$, $f_k^{(1)}$, and ϵ is

$$\begin{aligned} &\mathcal{R}_0(\epsilon + 2k\hbar\omega) f_k^{(0)} \\ &\quad = \sum_{k'} M_{k,k'}^{(ss)}(\epsilon) f_{k'}^{(0)} + \kappa_1^{-1} \sum_{k'} M_{k,k'}^{(sp)}(\epsilon) f_{k'}^{(1)}, \\ &\mathcal{R}_1[\epsilon + (2k+1)\hbar\omega] f_k^{(1)} \\ &\quad = \sum_{k'} M_{k,k'}^{(pp)}(\epsilon + \hbar\omega) f_{k'}^{(1)} + \kappa_1 \sum_{k'} M_{k',k}^{(sp)}(\epsilon) f_{k'}^{(0)}, \end{aligned} \tag{20}$$

where

$$M_{k,k'}^{(pp)}(\epsilon) = \bar{M}_{k,k'}^{(pp)}(\epsilon) + \hat{M}_{k,k'}^{(pp)}(\epsilon),$$

and the explicit forms of the matrix elements $M_{k,k'}^{(ss)}$, $M_{k,k'}^{(sp)}$, and $\hat{M}_{k,k'}^{(pp)}$ are given in the Appendix.

In contrast to the case of an initial s-state $\psi_0(\mathbf{r})$, for the case of an initial p-state $\psi_1(\mathbf{r})$ with $m = 0$, the coefficients $f_s^{(1)}$ are even, $f_{s=2k}^{(1)} \equiv f_k^{(1)}$ [and can be normalized by the condition $f_0^{(1)} = 1$], while the coefficients $f_s^{(0)}$ are odd: $f_{s=2k-1}^{(0)} \equiv f_k^{(0)}$. It may be shown that the matrix equations for these coefficients are given by the system of Eqs. (20) upon substituting there $\epsilon \to (\epsilon - \hbar\omega)$.

The solution of Eq. (20) for the complex quasienergy ϵ and the coefficients $f_k^{(l)}$ completely specifies the QQES $\Phi_\epsilon(\mathbf{r},t)$ in Eq. (14) for the TS TDER model. This QQES $\Phi_\epsilon(\mathbf{r},t)$ may be used in different applications, such as above-threshold ionization or HHG. Equations (14) and (15) show that complete information on the effects of the potential $U(r)$ [which are described in our model by the scattering phases $\delta_0(k)$ and $\delta_1(k)$] enters the QQES $\Phi_\epsilon(\mathbf{r},t)$ only through the Fourier coefficients $f_s^{(0)}$ and $f_s^{(1)}$, which therefore are the basic ingredients of the TDER theory. The specific difference between the SS and the TS TDER models is that the former involves only the single set of coefficients $f_s^{(0)}$ or $f_s^{(1,m)}$ (for a bound s or p state, respectively), with even index s, while for the latter both the even and odd Fourier-coefficients are nonzero. According to Eq. (17), these coefficients determine the population of Fourier harmonics $\Phi_{s\omega}(\mathbf{r})$ of the QQES wave function $\Phi_\epsilon(\mathbf{r},t)$

$$\Phi_{s\omega}(\mathbf{r}) = \frac{1}{T}\int_0^T e^{is\omega t}\Phi_\epsilon(\mathbf{r},t)\,dt, \tag{21}$$

at small r, $r_c \lesssim r \ll \kappa_l^{-1}$, where the effects of the potential $U(r)$ are most important. Therefore, for the TS TDER model, both the even ($s = 2n$) and odd ($s = 2n+1$) QQES harmonics $\Phi_{s\omega}(\mathbf{r})$ at small r are populated. This fact implies that the contribution of the small-r region, $r \lesssim \kappa_l^{-1}$, to the amplitudes for electric dipole transitions involving an odd number of photons [between QQES harmonics $\Phi_{s\omega}(\mathbf{r})$ with different s] should be suppressed in the SS TDER model [for which the Fourier coefficients $f_s^{(l)}$ are only even], whereas in the TS TDER model they are not. In particular, for the HHG process (in which the spontaneous emission of a harmonic photon can be considered as an electric dipole transition between QQES harmonics with $s = 2n+1$ and $s = 0$), this qualitative consideration implies that the amplitude of the Nth harmonic ($N = 2n+1$) within the TS TDER theory can involve a recombination amplitude that differs from the plane-wave result that enters the HHG amplitude in the SS TDER model. Moreover, one may expect that the coefficient $f_{s=N}^{(1)}$ [or $f_{s=N}^{(0)}$] can give a significant contribution to the amplitude for the Nth harmonic for the case of an initial bound s-state $\psi_0(\mathbf{r})$ [or p-state $\psi_1(\mathbf{r})$].

C. Approximate results for the coefficients $f_s^{(l)}$

A rigorous solution of the QQES problem even for our simplified atomic model requires the solution of the eigenvalue problem represented by the infinite system of linear Eqs. (20). While an exact solution of this problem can be performed only numerically, simple analytical approximations can be obtained in two limiting cases: the weak field case and the low-frequency field case. In the first case, perturbative (in F) expansions for the complex quasienergy ϵ and the Fourier coefficients $f_s^{(l)}$ can be obtained for a sufficiently weak field $\mathbf{F}(t)$ [i.e., such that $\xi = u_p/(\hbar\omega) \ll 1$, where $u_p = e^2F^2/(4m\omega^2)$ is the mean quiver energy of a free electron in the field $\mathbf{F}(t)$]. For both Brillouin-Wigner and Rayleigh-Schrödinger formulations of perturbation theory, in the TS TDER theory these expansions can be constructed similarly to those for the SS TDER theory [18,30]. In the second case, the field is assumed to have a sufficiently low frequency [i.e., such that $\xi \gg 1$ and $\hbar\omega \ll |E_0|$]. Moreover, in the low-frequency limit, two levels of approximation for taking into account the effects of the potential $U(r)$ are possible, as described below.

1. Keldysh approximation

In this approximation the potential $U(r)$ is taken into account only in the lowest nonvanishing order. More specifically, it consists in (i) approximating the quasienergy ϵ by the energy E_l of the initial bound state $\psi_l(\mathbf{r})$, $\epsilon \simeq E_l$, and (ii) neglecting all Fourier-coefficients $f_s^{(0)}$ and $f_s^{(1)}$ except $f_{s=0}^{(l)}$, that is,

$$\epsilon = E_l, \quad f_{s=0}^{(l)} = 1. \tag{22}$$

In this Keldysh approximation (KA) (22), the TS TDER results for the QQESs therefore reduce to the KA results for the SS TDER model involving only a single bound state $\psi_l(\mathbf{r})$, either $\psi_0(\mathbf{r})$ or $\psi_1(\mathbf{r})$. In particular, as was the case in the SS TDER model [31], in the low-frequency tunneling limit the ionization rate for the state $\psi_l(\mathbf{r})$ calculated within the KA (22) coincides with the Keldysh result for tunnel ionization [32], while the HHG rates coincide with those obtained in the SFA.

2. Rescattering approximation

The lowest-order results for the Fourier coefficients $f_s^{(0)}$ and $f_s^{(1)}$, which are omitted in the KA (22), originate from high-order effects of the potential $U(r)$. For an initial bound s-state, $\psi_0(\mathbf{r})$, approximate results for these coefficients can be obtained by an iterative solution of Eq. (20), approximating $\epsilon = E_0$ and considering the KA (22) as the zero iteration [i.e., substituting $f_{s=2k'}^{(0)} \equiv f_{k'}^{(0)} = \delta_{0,k'}$ and $f_{s=2k'+1}^{(1)} \equiv f_{k'}^{(1)} = 0$ on the right-hand side in Eq. (20)]. As a result, the coefficients $f_k^{(0)}$ and $f_k^{(1)}$ are approximated as follows:

$$\begin{aligned} f_0^{(0)} &= 1, \quad f_{k\neq 0}^{(0)} = \frac{M_{k,0}^{(ss)}(E_0)}{\mathcal{R}_0(E_0 + 2k\hbar\omega)}, \\ f_k^{(1)} &= \frac{\kappa_1 M_{0,k}^{(sp)}(E_0)}{\mathcal{R}_1[E_0 + (2k+1)\hbar\omega]}. \end{aligned} \tag{23}$$

For an initial bound p-state $\psi_1(\mathbf{r})$, the coefficients $f_{s=2k}^{(1)} \equiv f_k^{(1)}$ and $f_{s=2k-1}^{(0)} \equiv f_k^{(0)}$ are given by

$$\begin{aligned} f_0^{(1)} &= 1, \quad f_{k\neq 0}^{(1)} = \frac{M_{k,0}^{(pp)}(E_1)}{\mathcal{R}_1(E_1 + 2k\hbar\omega)}, \\ f_k^{(0)} &= \frac{\kappa_1^{-1} M_{k,0}^{(sp)}(E_1 - \hbar\omega)}{\mathcal{R}_0[E_1 + (2k-1)\hbar\omega]}. \end{aligned} \tag{24}$$

Figure 1 demonstrates the high accuracy of the rescattering approximation (RA). For the case of an initial s-state $\psi_0(\mathbf{r})$, the values of the coefficients $f_s^{(0)}$ and $f_s^{(1)}$ with increasing $|s|$ as calculated in the RA (23) are compared in Fig. 1 with the exact solutions of Eq. (20). The plateau-like structures in the dependence of $f_s^{(0)}$ and $f_s^{(1)}$ on s for $s > 0$ are similar to those for the SS TDER model [17,30]. In general, for both the $f_s^{(0)}$ and the $f_s^{(1)}$ coefficients, the plateau onset and the plateau cutoff values of s, s_o, and s_{cut} depend only on the energy E_l of the initial bound state $\psi_l(\mathbf{r})$

$$s_0 = \left[\frac{|E_l|}{\hbar\omega}\right], \quad s_{\text{cut}} = \left[\frac{|E_l| + 3.17u_p}{\hbar\omega}\right], \tag{25}$$

where $[x]$ is the integer part of x. For values of s in the vicinity of the plateau cutoff, Fig. 1 shows the excellent agreement of the exact results for $f_s^{(0)}$ and $f_s^{(1)}$ with those obtained using the RA (23).

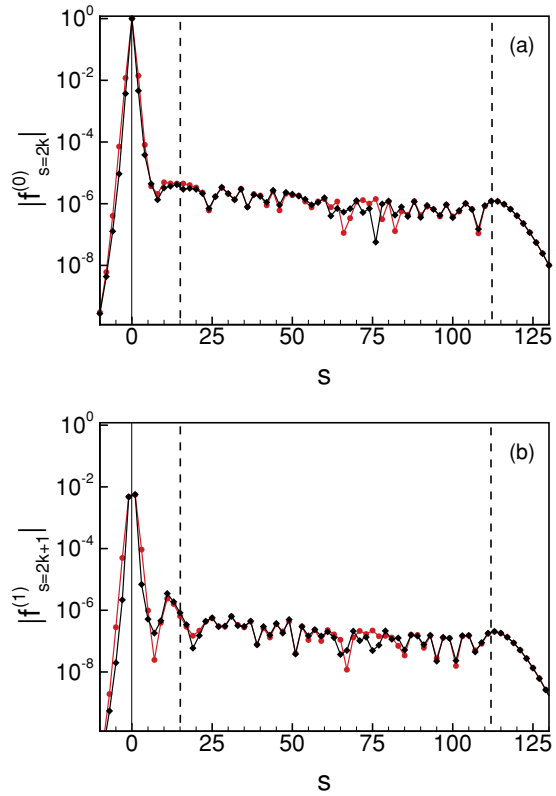

FIG. 1. (Color online) Comparison of rescattering approximation (RA) and exact results for the absolute values of the Fourier coefficients (a) $f_s^{(0)}$ and (b) $f_s^{(1)}$ of the TS TDER model QQES corresponding to an initially occupied s-state $\psi_0(\mathbf{r})$ for the model parameters $|E_0| = 12$ eV, $C_{\kappa_0} = 2$, $|E_1| = 3$ eV, and $C_{\kappa_1} = 0.35$ and the laser parameters $\lambda = 1600$ nm and $I = 10^{14}$ W/cm^2. Circles (joined by red lines): exact TS TDER results [according to Eq. (20)]; diamonds (joined by black lines): the RA results [Eq. (23)]. Vertical dashed lines mark the positions of the plateau onset and cutoff s_o and s_{cut} [Eq. (25)]. The red and black solid lines have been added to guide the eye.

III. HHG AMPLITUDES AND RATES WITHIN THE TS TDER THEORY

A. Exact TS TDER results

Using the rigorous formulation of Ref. [33] for the amplitude of the Nth harmonic $\chi_N(F,\omega)$ in terms of the complex quasienergy of a quantum system in two laser fields (i.e., an intense driving laser field of frequency ω and a weak probe laser field of frequency $N\omega$), analytic results for $\chi_N(F,\omega)$ within the TS TDER theory can be obtained by generalizing the similar derivation for $\chi_N(F,\omega)$ within the SS TDER model [34]. We find that the same results are obtained upon using the definition for $\chi_N(F,\omega)$ in terms of the Fourier component

$$\chi_N(F,\omega) = \frac{1}{T}\int_0^T e^{iN\omega t}\mathbf{e}_z \cdot \tilde{\mathbf{d}}(t)\,dt, \quad \mathbf{e}_z = \mathbf{F}/F, \tag{26}$$

of the dual dipole moment

$$\tilde{\mathbf{d}}(t) = \langle \tilde{\Phi}_\epsilon(\mathbf{r},t)|e\mathbf{r}|\Phi_\epsilon(\mathbf{r},t)\rangle, \tag{27}$$

where $\Phi_\epsilon(\mathbf{r},t)$ is the exact QQES wave function (14), and $\tilde{\Phi}_\epsilon(\mathbf{r},t)$ is its dual wave function [30], defined by

$$\tilde{\Phi}_\epsilon(\mathbf{r},t) \equiv \Phi^*_\epsilon(\mathbf{r},-t)|_{m\to -m}. \tag{28}$$

Since $\Phi_\epsilon(\mathbf{r},t)$ [cf. Eq. (14)] contains two terms (with $l=0$ and 1) related to the ground (ψ_0) and excited (ψ_1) states, the amplitude $\chi_N(F,\omega)$ comprises four components corresponding to contributions from ψ_0 (χ_N^{ss}), ψ_1 (χ_N^{pp}), and their associated cross terms (χ_N^{sp} and χ_N^{ps}). For arbitrary parameters F, ω, and $|E_0|$, the exact analytic expressions of these components are cumbersome since they involve double summations over the Fourier coefficients $f_s^{(0)}$ and $f_s^{(1)}$ (cf. similar, though simpler, results for the SS TDER model in Ref. [34]). However, for a low-frequency field ($\hbar\omega \ll |E_l|$) in the tunneling limit [$\gamma = \hbar\omega/(|e|F\kappa_l^{-1}) \ll 1$, where γ is the Keldysh parameter [32]], we find numerically that the dominant contributions to $\chi_N(F,\omega)$ stem from fewer terms. Thus, for an initial bound s-state $\psi_0(\mathbf{r})$, the dominant contributions originate from χ_N^{ss} and the cross term χ_N^{sp}

$$\chi_N(F,\omega) \simeq \chi_N^{KA}(F,\omega) + \bar{\chi}_N(F,\omega), \tag{29}$$

where χ_N^{KA} is the KA result [i.e., that obtained from the QQES wave function (14) upon substituting there $f^{(0)}(t)=1$, $f^{(1)}(t)=0$, and $\epsilon = E_0$]. This KA result originates from the component χ_N^{ss} and coincides with that in the SS TDER theory for a single s state [34]

$$\chi_N^{KA}(F,\omega) = \mathcal{C}_0 \int_0^\infty \frac{d\tau}{\tau^{3/2}} e^{2iE_0\tau/(\hbar\omega) - i\lambda(\tau)} \times \{j_-(\tau)J_{(N-1)/2}[z(\tau)] - ij_+(\tau)J_{(N+1)/2}[z(\tau)]\}, \tag{30}$$

where

$$j_\pm(\tau) = \frac{\sin\tau\sin(N\tau)}{\tau} - \frac{N\sin[(N\pm 1)\tau]}{N\pm 1}, \qquad \mathcal{C}_0 = -i^{N/2}\frac{eC_{\kappa_0}^2}{\kappa_0 N^2}\frac{|E_0|}{\hbar\omega}\sqrt{\frac{u_p}{\pi\hbar\omega}}, \tag{31}$$

and $z(\tau)$ and $\lambda(\tau)$ are given by Eqs. (A5) and (A6).

The amplitude $\bar{\chi}_N(F,\omega)$ originates from the cross term χ_N^{sp} upon substituting therein $f_s^{(0)} = \delta_{s,0}$ and $f_s^{(1)} = f_N^{(1)}$. This amplitude describes the contribution of the excited p-state and the p-wave continuum channel to the emission of the Nth harmonic by the active electron that is bound initially in the ground s state. Its analytic form (approximating $\epsilon = E_0$) is

$$\bar{\chi}_N(F,\omega) = f_{s=N}^{(1)} D_N(F,\omega), \tag{32}$$

where

$$D_N(F,\omega) = \mathcal{C}_1 \int_0^\infty \frac{d\tau}{\tau^{3/2}} e^{2i[E_0/(\hbar\omega)+N/2]\tau - i\lambda(\tau)} \times \left[\frac{u_p}{N\hbar\omega}\{[j_-(\tau)\zeta_-(\tau) + j_+(\tau)\zeta_+(\tau)]J_0[z(\tau)] - i[j_+(\tau)\zeta_-(\tau) + j_-(\tau)\zeta_+(\tau)]J_1[z(\tau)]\} - \frac{i}{2}\zeta_N(\tau)J_0[z(\tau)]\right], \tag{33}$$

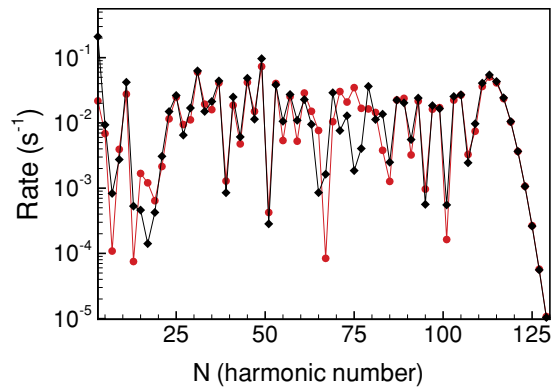

FIG. 2. (Color online) Comparison of exact TS TDER results for HHG rates (circles joined by red lines) with those given by the approximation (29) for χ_N (diamonds joined by black lines). The atomic model and laser parameters are the same as in Fig. 1.

in which

$$\zeta_N(\tau) = e^{-iN\tau} - \frac{\sin N\tau}{N\tau}, \qquad \mathcal{C}_1 = -i^{1/2}\frac{eC_{\kappa_0}^2}{\kappa_1 N}\sqrt{\frac{3|E_0|}{2\pi\hbar\omega}},$$

and the functions $\zeta_\pm(\tau)$ are given by Eq. (A7).

In the high-energy region of the HHG plateau, the high accuracy of the HHG rates $\mathcal{R}_N$

$$\mathcal{R}_N = \frac{\Omega^3}{2\pi\hbar c^3}|\chi_N(F,\omega)|^2, \tag{34}$$

calculated using the approximation (29) for $\chi_N(F,\omega)$, is shown in Fig. 2 by comparison with exact numerical TS TDER results for $\chi_N(F,\omega)$ for an initial state $\psi_0(\mathbf{r})$.

B. Factorization of HHG amplitudes and rates in the high-energy plateau region

Although the approximation (29) for the HHG amplitude is accurate in the low-frequency limit, the exact expressions for its two components (30) and (32) (which are valid for any frequency) involve complicated integrals of Bessel functions. Moreover, in general, the coefficient $f_{s=N}^{(1)}$ in Eq. (32) can be calculated only numerically. Approximate analytic results for low frequencies ($\hbar\omega \ll |E_0|$) can be obtained using the quasiclassical approximation for HHG amplitudes in the TDER theory that was developed in Ref. [34]. An analytic result (in terms of the Airy function) for the KA amplitude χ_N^{KA} (30) in this approximation was obtained in Ref. [14]. It thus remains for us to analyze $\bar{\chi}_N(F,\omega)$ in Eq. (32) [i.e., we must estimate $f_{s=N}^{(1)}$ and D_N].

The coefficients $f_s^{(1)}$ are highly sensitive to the field amplitude F in the strong field regime and decrease $\sim F^s$ as $F\to 0$ (cf. Ref. [30]). In contrast, D_N is not: We find numerically that for small ω the integral in Eq. (33) depends only weakly on F and, as shown numerically in Fig. 3, this integral may be approximated by its value at $F=0$, which is

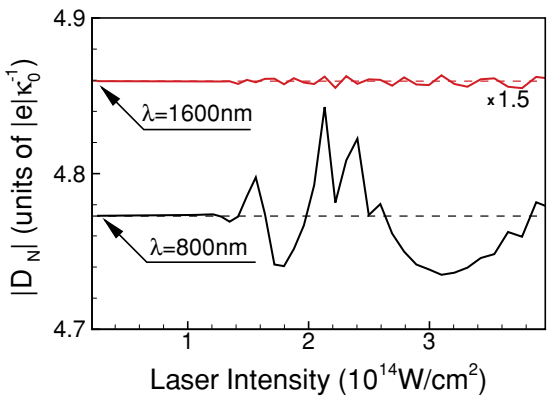

FIG. 3. (Color online) Comparison of the exact result (33) for the absolute value of $D_N(F,\omega)$ (solid lines) with the approximation (35) (dashed lines), in units of $|e|\kappa_0^{-1} = 1.065|e|a_B$. Black lines: results for the 21st harmonic of a laser field with $\lambda = 800$ nm; red lines: results for the 113th harmonic of a laser field with $\lambda = 1600$ nm (with these latter results multiplied by a factor 1.5). The parameters of the atomic model are the same as in Fig. 1.

easily calculated analytically

$$D_N(F=0,\omega) = \frac{e\kappa_0 C_{\kappa_0}^2}{\sqrt{3}\kappa_1}\frac{\kappa_0 - 2ik}{(\kappa_0 - ik)^2}, \tag{35}$$

where $k = \sqrt{2mE}/\hbar$, $E = N\hbar\omega - |E_0|$. The origin of this surprisingly weak dependence of $D_N(F,\omega)$ on F becomes clear upon evaluating the exact expression for $\bar{\chi}_N(F,\omega)$ in Eq. (32), which has the following form:

$$\bar{\chi}_N(F,\omega) = \left\langle \tilde{\Phi}_0^{(l=0)}(\mathbf{r})|ez|\Phi_{N\omega}^{(l=1)}(\mathbf{r})\right\rangle, \tag{36}$$

where $\tilde{\Phi}_0^{(l=0)}(\mathbf{r})$ $[= \Phi_0^{(l=0)*}(\mathbf{r})]$ and $\Phi_{N\omega}^{(l=1)}(\mathbf{r})$ are Fourier harmonics [cf. Eq. (21)] of constituents of the QQES $\Phi_\epsilon(\mathbf{r},t)$ in Eq. (14) corresponding to s (ψ_0) and p (ψ_1) states. Additionally, in the expression for $\Phi_{N\omega}^{(l=1)}(\mathbf{r})$ we take into account only the term involving $f_{s=N}^{(1)}$, as in Eq. (32). To estimate $\bar{\chi}_N(F,\omega)$, we take into account only the s-wave and p-wave components of $\Phi_0^{(l=0)}(\mathbf{r})$ and $\Phi_{N\omega}^{(l=1)}(\mathbf{r})$, which give the dominant contributions to the dipole matrix element (36). Moreover, we approximate these components neglecting laser-induced corrections, which are small for $F < F_0$, where $F_0 = \sqrt{8m|E_0|^3}/(|e|\hbar) = |e|a_B\kappa_0^3$. In this approximation, $\Phi_0^{(l=0)}(\mathbf{r})$ reduces to the ground state $\psi_0(\mathbf{r})$ in Eq. (6), while $\Phi_{N\omega}^{(l=1)}(\mathbf{r})$ takes the form

$$\Phi_{N\omega}^{(l=1)}(\mathbf{r}) \approx i f_N^{(1)} C_{\kappa_0}\sqrt{\kappa_0}\kappa_1^{-1}k^2 h_1^{(1)}(kr)Y_{10}(\hat{\mathbf{r}}). \tag{37}$$

The analytic calculation of the matrix element in Eq. (36) using $\psi_0(\mathbf{r})$ instead of $\tilde{\Phi}_0^{(l=0)}(\mathbf{r})$ and the approximation (37) for $\Phi_{N\omega}^{(l=1)}(\mathbf{r})$ reproduces the result (32) for $\bar{\chi}_N(F,\omega)$ with $D_N(F,\omega)$ given by Eq. (35) once again.

To estimate analytically the odd Fourier coefficient $f_{s=2k+1}^{(1)}$ in Eq. (32) in the limit $\hbar\omega \ll |E_0|$, we use the RA (23) and the quasiclassical estimate for the matrix element $M_{0,k}^{(sp)}(E_0)$, which can be derived by generalizing the techniques used to estimate the even Fourier coefficients $f_{s=2k}$ in the SS TDER theory (cf. Eq. (21) in Ref. [35])

$$M_{0,k}^{(sp)}(E_0) = i\frac{\sqrt{3}m\omega^4}{2\pi^2 e\hbar F}\sum_n \sqrt{\frac{2\pi i\hbar}{S''(p_n,t_0)}} \times \int_0^T dt \frac{e^{i(2k+1)\omega t - i[S(p_n,t)-S(p_n,t_0)]/\hbar}}{|\cos\omega t - \cos\omega t_0|}(p_n - p_t), \tag{38}$$

where $p_n = \sqrt{2m(E_0 - u_p + n\hbar\omega)}$

$$p_t = \frac{eF}{\omega}\sin\omega t, \quad S''(p_n,t_0) = \frac{\partial^2}{\partial t_0^2}S(p_n,t_0),$$

and $S(p_n,t)$ is the classical action of an electron with momentum $\mathbf{p}_n = \mathbf{e}_z p_n$ in the field $\mathbf{F}(t) = \mathbf{e}_z F\cos\omega t$

$$S(p_n,t) = \int^t \left[\frac{(\mathbf{p}_n - \mathbf{e}_z p_\tau)^2}{2m} - E_0\right]d\tau.$$

The time t_0 in Eq. (38) is that root of the saddle-point equation, $\partial S(p_n,t_0)/\partial t_0 = 0$, which has both a positive imaginary part and the smallest value of Re t_0 [35]. An approximate evaluation of the sum and integral in Eq. (38), valid in the tunneling limit ($\gamma \ll 1$), can be performed similarly to that for the KA amplitude χ_N^{KA} in Ref. [14].

The result of these various estimations is the following closed-form analytic expression for $f_{s=N}^{(1)}$ in the RA:

$$f_{s=N}^{(1)RA} = -\sqrt{3}C_{\kappa_0}^2 e^{i\Phi_0}\frac{\hbar\omega}{|E_0|}\sqrt{\frac{F_0}{\tilde{F}}}e^{-F_0/(3\tilde{F})} \times \frac{\mathrm{Ai}(\xi)}{\zeta^{1/3}(v_{\mathrm{at}}\Delta t)^{3/2}}\frac{k\kappa_1\sqrt{a_B}}{\mathcal{R}_1(E)}, \tag{39}$$

where $v_{\mathrm{at}} = e^2/\hbar$, the phase Φ_0 is given by the classical action of an electron moving in the field $\mathbf{F}(t)$ from the moment of (tunnel) ionization $t_i = -0.45T$ up to the time of recombination $t_r = 0.2T$ (for the explicit form of Φ_0 see Ref. [14]); $\tilde{F} = F|\cos\omega t_i| \simeq 0.951F$ is an effective static electric field given by the instantaneous value of $\mathbf{F}(t)$ at the moment of ionization; $\Delta t = t_r - t_i = 4.086\omega^{-1} = 0.65T$ is the return time of the electron for the shortest closed classical trajectory in the field $\mathbf{F}(t)$ along which an electron with zero initial momentum gains the maximum classical energy $\mathcal{E}_{\max}^{(\mathrm{cl})}$ from the field $\mathbf{F}(t)$. The argument of the Airy function $\mathrm{Ai}(\xi)$ in Eq. (39) is

$$\xi = \frac{E - \mathcal{E}_{\max}}{\zeta^{1/3}E_{\mathrm{at}}}, \quad \zeta = \delta\frac{I}{I_{\mathrm{at}}}, \tag{40}$$

where $I = cF^2/(8\pi)$, $I_{\mathrm{at}} = 3.51\times 10^{16}$ W/cm^2, $E_{\mathrm{at}} = 27.21$ eV, and $\mathcal{E}_{\max} = \mathcal{E}_{\max}^{(\mathrm{cl})} + \Delta|E_0|$, where $\Delta|E_0|$ is the lowest-order quantum correction to $\mathcal{E}_{\max}^{(\mathrm{cl})}$ [14,36]. The energy $\mathcal{E}_{\max}^{(\mathrm{cl})}$ and the dimensionless parameters Δ and δ can all be expressed explicitly in terms of a single parameter, the dimensionless return time, $\tilde{\tau} = \omega\Delta t = 4.086$ [37]

$$\begin{aligned}\mathcal{E}_{\max}^{(\mathrm{cl})} &= 4u_p\sin^2(\tilde{\tau}/2) \approx 3.17u_p,\\ \Delta &= \cot(\tilde{\tau}/2 - \pi/4) \approx 0.324,\\ \delta &= \tfrac{1}{4}(\Delta^2 + \Delta - \tilde{\tau})\cos\tilde{\tau} \approx 0.536.\end{aligned} \tag{41}$$

Multiplying the result (39) for $f_{s=N}^{(1)\mathrm{RA}}$ by the expression (35) for D_N and adding the KA amplitude $\chi_N^{KA}(F,\omega)$ in the tunneling limit [the explicit form of which is given in Ref. [14]; it is very similar to the expression (39)], the final RA result for the HHG amplitude (29) is

$$\chi_N^{\mathrm{RA}}(F,\omega) = -eC_{\kappa_0}^2 e^{i\Phi_0}\kappa_0\sqrt{a_B}\frac{\hbar\omega}{|E_0|}\sqrt{\frac{F_0}{\tilde{F}}}e^{-F_0/(3\tilde{F})}\frac{\mathrm{Ai}(\xi)}{\zeta^{1/3}(v_{\mathrm{at}}\Delta t)^{3/2}} \times\left[\frac{2k}{(k^2+\kappa_0^2)^2}+\frac{k}{\mathcal{R}_1(E)}\frac{\kappa_0-2ik}{(\kappa_0-ik)^2}\right]. \tag{42}$$

Equation (42) is the key result of this paper. It shows that the term in square brackets is (up to a numerical factor) the exact amplitude for photorecombination to the state $\psi_0(\mathbf{r})$ given by Eq. (11). Our derivations show clearly the origin of this amplitude in our quantum treatment of HHG: the first plane-wave term in square brackets in Eq. (42) originates from the KA part of the HHG amplitude (29) [i.e., it corresponds to treating the potential $U(r)$ in lowest nonvanishing order, as in the SFA or SS TDER model], while the second term [proportional to $\mathcal{R}_1^{-1}(E)$] originates from higher-order contributions of the potential $U(r)$ [such as the distortion of the p-wave continuum channel by the potential $U(r)$ and the existence of an excited p state] that are omitted in the KA (22) and are described by the next-order (RA) corrections (23) to the KA.

Substituting $\chi_N^{\mathrm{RA}}(F,\omega)$ from (42) into Eq. (34), we reproduce the factorization formula (1), in which $\sigma_{\mathrm{rec}}(E)$ is given by Eqs. (9) and (11), while the explicit form of the EWP $W(E)$ is given by the product of ionization ($\mathcal{I}$) and propagation ($\mathcal{W}$) factors, which are the same as in the SS TDER model [15]

$$W(E) = \mathcal{I}(\tilde{F},\omega)\mathcal{W}(E), \tag{43}$$

$$\mathcal{I}(\tilde{F},\omega) = \kappa_0 a_B C_{\kappa_0}^2\tilde{\gamma}^2\frac{\tilde{F}}{\pi F_0}e^{-2F_0/(3\tilde{F})}, \tag{44}$$

$$\mathcal{W}(E) = \frac{p}{m}\frac{\mathrm{Ai}^2(\xi)}{\zeta^{2/3}(v_{\mathrm{at}}\Delta t)^3}, \tag{45}$$

where $\tilde{\gamma} = \hbar\omega/(|e|\tilde{F}\kappa_0^{-1})$ and $p = \sqrt{2mE}$.

In Fig. 4 we present a comparison of the exact TS TDER results for HHG rates with approximate RA and KA results for the two-state model system (with $|E_0| = 12$ eV, $C_{\kappa_0} = 2$ and $|E_1| = 3$ eV, $C_{\kappa_1} = 0.35$) for two sets of laser parameters. In both cases one observes excellent agreement between the exact and the RA results in the region of the high-energy plateau cutoff and beyond. On the other hand, the KA results, which neglect the p-wave scattering phase $\delta_{l=1}(k)$ (or, equivalently, use the plane-wave results for the photorecombination cross section), overestimate considerably the exact results for the HHG rates. Since our factorized result for HHG rates was derived in the tunneling limit, $\gamma \ll 1$, the interval of its applicability for harmonic energies below the plateau cutoff increases with decreasing Keldysh parameter γ or, equivalently, with increasing ratio $u_p/|E_0|$ [$= (2\gamma^2)^{-1}$]. This is confirmed by the results in Fig. 4, where $\gamma = 0.5$ and 0.25 for Figs. 4(a) and 4(b), respectively.

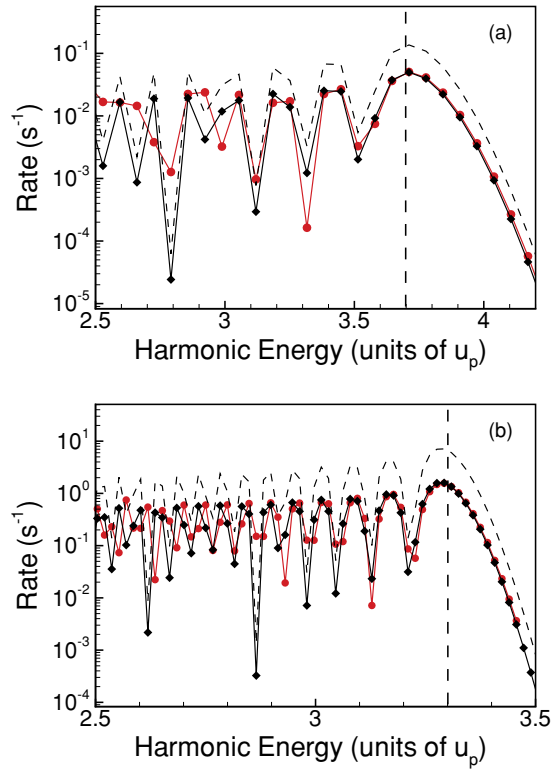

FIG. 4. (Color online) Comparison of exact TS TDER theory results for HHG rates with approximate RA and KA results in the energy region of the HHG plateau cutoff for the same atomic model and laser wavelength as in Fig. 1 for two different laser intensities: (a) $I = 1\times10^{14}$ W/cm^2 ($u_p = 23.6$ eV) and (b) $I = 4\times10^{14}$ W/cm^2 ($u_p = 94.4$ eV). Circles (joined by red lines): exact TS TDER results; diamonds (joined by black lines): RA results [Eq. (42)]; dashed lines: KA results [which neglect the term proportional to $\mathcal{R}_1^{-1}(E)$ in Eq. (42)]. Vertical dashed lines mark the classical cutoff position at $|E_0| + 3.17u_p$.

Finally, we note that the general results of the TS TDER theory in Sec. II are equally applicable to the case of an initial s or p state, while our derivations for the HHG amplitude and rates in this Sec. III have been performed only for an initial s state. These results are valid also for a negative scattering length a_1, in which case the bound p state does not exist. For an initially populated bound p state with angular momentum projection $m = 0$, all derivations are very similar and yield the factorized result (1) for the HHG rates, in which the photorecombination cross section $\sigma_{\mathrm{rec}}(E)$ to the bound p state is given by the exact results (9) and (12) for the TS TDER model.

IV. DISCUSSION AND CONCLUSION

In common analytic theories of HHG, such as the Lewenstein *et al.* model [36] or the SFA within the S-matrix theory [25], the structure of a particular atomic target is taken into account only on the level of the ground-state wave function of the active atomic electron. Following its ionization by tunneling, the influence of the atomic potential $U(r)$ on the active electron's subsequent motion (in accordance with the well-known three-step HHG scenario [9,10]) is neglected (i.e.,

the active electron in the laser-dressed continuum is treated as free). This approximation is completely similar to that in the Keldysh theory for tunnel ionization [32], in which case the absence of a high-energy plateau in the energy spectra of tunneling electrons results from neglecting atomic potential effects in the continuum.

The SS TDER model [17] provides a more precise account of the potential $U(r)$. This model is oversimplified because on the field-free level it assumes that the potential $U(r)$ supports only a single bound state with angular momentum l, which is a realistic assumption only for a negative ion. This bound state, however, dynamically interacts with the continuum through a nonzero scattering phase in the l-wave channel $\delta_l(k)$. As a result, this single-state model presents a rare case (probably unique) of a self-consistent, three-dimensional, exactly-solvable quantum model in strong laser-atom physics. Moreover, this model predicts a number of qualitative features of HHG and other strong field processes that are observable not only for negative ions but also for neutral atoms. In particular, the solution of the QQES problem for the SS TDER model [which is nonperturbative in both $U(r)$ and the electron-laser interaction (13)] predicts the high-energy plateau in above-threshold ionization (ATI). (The description of this ATI plateau within the SFA requires an additional (perturbative) account of the potential $U(r)$ [25].) Use of the SS TDER theory also allowed us to derive analytically a factorized result [similar to Eq. (1)] for ATI rates in the high-energy part of the ATI plateau; one of the factors is the exact differential cross section for elastic electron scattering from the potential $U(r)$ in the l-wave channel [35].

However, none of the existing analytic theories of HHG allows one to derive a factorized result for HHG rates involving the exact (non-Born) result for the recombination cross section $\sigma_{\rm rec}$, thereby providing a theoretical justification for the phenomenological factorization formula (1). Compared to ATI, for HHG an additional difficulty in treating atomic potential effects beyond the lowest nonvanishing order is that, owing to dipole selection rules, $\sigma_{\rm rec}$ involves the phases $\delta_{l\pm1}(k)$ of electron scattering from the potential $U(r)$, where l is the angular momentum of the active atomic electron in the initial bound state. Therefore, the exact result for $\sigma_{\rm rec}$, in principle, cannot enter HHG rates either by treating $U(r)$ perturbatively, as in the improved SFA, or in the SS TDER theory, in which the action of the potential $U(r)$ on the continuum electron is treated nonperturbatively only in a single l-wave channel [i.e., the scattering phase $\delta_l(k)$ is nonzero, but $\delta_{l\pm1}(k) = 0$]. To overcome this deficiency of the SS TDER model and to account more precisely for the effects of the potential $U(r)$ in strong field processes, in this paper we have formulated TDER theory for the case of a potential $U(r)$ supporting two bound states with opposite parities (s and p) to ensure the laser-induced electric-dipole coupling between the s- and p-wave continuum channels in the presence of a laser field. This TS TDER theory shows that the inclusion of an excited state (thus approximating better the states of an electron in a neutral atom) and the distortion of more than one partial-wave continuum channel by the potential $U(r)$ significantly modify the structure of the Fourier harmonics $\Phi_{s\omega}(\mathbf{r})$ of the exact QQES wave function as compared to the case of a single-level model. The most significant difference is a nonzero population of two branches of QQES harmonics $\Phi_{s\omega}(\mathbf{r})$ at small distances r (i.e., those with even and odd s having, respectively, opposite spatial parities). [In the SS TDER model, only QQES harmonics with even s are populated at the origin [17], while for any realistic atomic potential, of course, both even and odd QQES-harmonics $\Phi_{s\omega}(\mathbf{r})$ are populated at small r.] Consequently, the TS TDER HHG amplitude $\chi_N(F,\omega)$ in the tunneling limit can be approximated by a sum of two components having very different origin: one originates from the QQES harmonic $\Phi_{N\omega}(\mathbf{r})$ taking into account the potential $U(r)$ in the lowest nonvanishing order (i.e., on the level of the ground-state wave function) as in the SFA; the other originates from contributions of the excited p-state and p-wave continuum channel to the harmonic $\Phi_{N\omega}(\mathbf{r})$ at small r. As we have shown, the proper analytic evaluation of these two components in the tunneling limit yields the result for their sum $\chi_N(F,\omega)$ that involves, as a factor, the exact TS TDER result for the photorecombination amplitude. It is important to emphasize that our two-channel modification of the SS TDER theory results only in the modification of the photorecombination cross section, while the EWP $W(E)$ in Eq. (43) remains the same as in the SS TDER theory [15] (i.e., it involves only the parameters $|E_0|$ and C_{κ_0} of the initial bound state). Thus, our results in this paper explain the weak sensitivity of the EWP $W(E)$ in Eq. (1) to the details of the atomic structure, as has been found experimentally and in numerical simulations [11–13].

To conclude, we have shown theoretically that, in the tunneling limit, HHG rates within the TS TDER model indeed have the form (1) with the exact photorecombination cross section $\sigma_{\rm rec}$. Our results are valid for harmonics with energies in the region of the HHG plateau cutoff and beyond, which are precisely the ones used to produce attosecond pulses. Our model considerations show that, with a proper account of excited and continuum states of the electron in the potential $U(r)$, the parametrization (1) can be derived analytically, by estimating the exact quantum results for the HHG amplitude. Therefore, it is reasonable to expect that, in general (in the tunneling limit), atomic structure effects on HHG with harmonic energies around and at the plateau cutoff are also incorporated within a single field-free atomic parameter $\sigma_{\rm rec}$. Thus the results in this paper confirm our analytic expression [15] of the three-step scenario for HHG [9,10] involving the exact, atom-specific photorecombination cross section and explain why the phenomenological parametrization (1) is in excellent agreement with both experimental and numerical data. Finally, we note that the laser frequency ω in this paper was assumed to be nonresonant to the transition between the ground and excited states. Another advantage of the TS TDER theory, not discussed in this paper, is the possibility of an analytic description of a number of qualitative features in resonant HHG processes, which will be published elsewhere.

ACKNOWLEDGMENTS

This work was supported, in part, by the Russian Foundation for Basic Research under Grant No. 10-02-00235, by NSF Grant No. PHY-0901673, and by the "Dynasty" Foundation (T.S.S.).

APPENDIX: EXPLICIT FORM OF THE MATRIX ELEMENTS IN Eqs. (19) AND (20)

The matrix elements that appear in Eqs. (19) and (20) have the following explicit forms:

$$\bar{M}^{(pp)}_{k,k'}(\epsilon) = -\frac{i}{2}\mathcal{C}\int_0^\infty d\tau \frac{e^{2i\tilde{\epsilon}_{kk'}\tau}}{\tau^{5/2}}\{e^{-i\lambda(\tau)}J_{k-k'}[z(\tau)] - \delta_{k,k'}\}, \quad \text{(A1)}$$

$$M^{(ss)}_{k,k'}(\epsilon) = \frac{\varkappa^2\mathcal{C}}{3}\int_0^\infty d\tau \frac{e^{2i\tilde{\epsilon}_{kk'}\tau}}{\tau^{3/2}}\{e^{-i\lambda(\tau)}J_{k-k'}[z(\tau)] - \delta_{k,k'}\}, \quad \text{(A2)}$$

$$M^{(sp)}_{k,k'}(\epsilon) = \varkappa\sqrt{\frac{u_p}{3\hbar\omega}}\mathcal{C}\int_0^\infty d\tau \frac{e^{i[2\tilde{\epsilon}_{kk'}+1]\tau - i\lambda(\tau)}}{\tau^{3/2}} \times \{\zeta_-(\tau)J_{k-k'}[z(\tau)] + i\zeta_+(\tau)J_{k-k'-1}[z(\tau)]\}, \quad \text{(A3)}$$

$$\hat{M}^{(pp)}_{k,k'}(\epsilon) = 2\frac{u_p}{\hbar\omega}\mathcal{C}\int_0^\infty d\tau \frac{e^{2i\tilde{\epsilon}_{kk'}\tau - i\lambda(\tau)}}{\tau^{3/2}} \times \{v_-(\tau)J_{k-k'}[z(\tau)] + i v_+(\tau)J'_{k-k'}[z(\tau)]\}, \quad \text{(A4)}$$

where the following notations are used:

$$z(\tau) = \frac{2u_p}{\hbar\omega}\sin\tau\left(\cos\tau - \frac{\sin\tau}{\tau}\right), \quad \text{(A5)}$$

$$\lambda(\tau) = \frac{2u_p}{\hbar\omega}\left(\tau - \frac{\sin^2\tau}{\tau}\right), \quad \text{(A6)}$$

$$\zeta_\pm(\tau) = e^{\pm i\tau} - \frac{\sin\tau}{\tau}, \quad \text{(A7)}$$

$$v_\pm(\tau) = \left(\cos\tau - \frac{\sin\tau}{\tau}\right)^2 \pm \sin^2\tau, \quad \text{(A8)}$$

$$\tilde{\epsilon}_{kk'} = \frac{\epsilon}{\hbar\omega} + k + k', \quad \mathcal{C} = \frac{3\,i^{k-k'}}{\varkappa^3\sqrt{4\pi i}}, \quad \varkappa = \sqrt{\frac{\hbar}{m\omega}}. \quad \text{(A9)}$$

[1] Z. Chang, A. Rundquist, H. Wang, M. M. Murnane, and H. C. Kapteyn, Phys. Rev. Lett. **79**, 2967 (1997).
[2] Ch. Spielmann, N. H. Burnett, S. Sartania, R. Koppitsch, M. Schnürer, C. Kan, M. Lenzner, P. Wobrauschek, and F. Krausz, Science **278**, 661 (1997).
[3] E. J. Takahashi, T. Kanai, K. L. Ishikawa, Y. Nabekawa, and K. Midorikawa, Phys. Rev. Lett. **101**, 253901 (2008).
[4] M.-C. Chen, P. Arpin, T. Popmintchev, M. Gerrity, B. Zhang, M. Seaberg, D. Popmintchev, M. M. Murnane, and H. C. Kapteyn, Phys. Rev. Lett. **105**, 173901 (2010).
[5] P. Agostini and L. F. DiMauro, Rep. Prog. Phys. **67**, 813 (2004).
[6] F. Krausz and M. Ivanov, Rev. Mod. Phys. **81**, 163 (2009).
[7] J. Itatani, J. Levesque, D. Zeidler, H. Niikura, H. Pépin, J. C. Kieffer, P. B. Corkum, and D. M. Villeneuve, Nature (London) **432**, 867 (2004).
[8] J. Levesque, D. Zeidler, J. P. Marangos, P. B. Corkum, and D. M. Villeneuve, Phys. Rev. Lett. **98**, 183903 (2007).
[9] K. J. Schafer, B. Yang, L. F. DiMauro, and K. C. Kulander, Phys. Rev. Lett. **70**, 1599 (1993).
[10] P. B. Corkum, Phys. Rev. Lett. **71**, 1994 (1993).
[11] T. Morishita, A. T. Le, Z. Chen, and C. D. Lin, Phys. Rev. Lett. **100**, 013903 (2008).
[12] A. T. Le, T. Morishita, and C. D. Lin, Phys. Rev. A **78**, 023814 (2008).
[13] C. D. Lin, A. T. Le, Z. Chen, T. Morishita, and R. Lucchese, J. Phys. B **43**, 122001 (2010).
[14] M. V. Frolov, N. L. Manakov, T. S. Sarantseva, and A. F. Starace, J. Phys. B **42**, 035601 (2009).
[15] M. V. Frolov, N. L. Manakov, T. S. Sarantseva, M. Yu. Emelin, M. Yu. Ryabikin, and A. F. Starace, Phys. Rev. Lett. **102**, 243901 (2009).
[16] N. L. Manakov, V. D. Ovsiannikov, and L. P. Rapoport, Phys. Rep. **141**, 319 (1986).
[17] M. V. Frolov, N. L. Manakov, E. A. Pronin, and A. F. Starace, Phys. Rev. Lett. **91**, 053003 (2003).
[18] M. V. Frolov, N. L. Manakov, and A. F. Starace, Phys. Rev. A **78**, 063418 (2008).
[19] S. Minemoto, T. Umegaki, Y. Oguchi, T. Morishita, A. T. Le, S. Watanabe, and H. Sakai, Phys. Rev. A **78**, 061402(R) (2008).
[20] H. J. Wörner, H. Niikura, J. B. Bertrand, P. B. Corkum, and D. M. Villeneuve, Phys. Rev. Lett. **102**, 103901 (2009).
[21] R. A. Ganeev, J. Phys. B **40**, R213 (2007).
[22] R. A. Ganeev, Usp. Fiz. Nauk **179**, 65 (2009); Phys. Usp. **52**, 55 (2009).
[23] M. V. Frolov, N. L. Manakov, and A. F. Starace, Phys. Rev. A **82**, 023424 (2010).
[24] A. D. Shiner, B. E. Schmidt, C. Trallero-Herrero, H. J. Wörner, S. Patchkovskii, P. B. Corkum, J.-C. Kieffer, F. Légaré, and D. M. Villeneuve, Nature Phys. (Published online: 06 March 2011 doi:10.1038/nphys1940).
[25] W. Becker, F. Grasbon, R. Kopold, D. B. Milošević, G. G. Paulus, and H. Walther, Adv. At. Mol. Opt. Phys. **48**, 35 (2002).
[26] L. D. Landau and E. M. Lifshitz, *Quantum Mechanics: Non-Relativistic Theory*, 3rd ed. (Pergamon, Oxford, 1977), pp. 132–133.
[27] A. I. Baz', Ya. B. Zel'dovich, and A. M. Perelomov, *Scattering, Reactions, and Decays in Nonrelativistic Quantum Mechanics*, 2nd ed. (Nauka, Moscow, 1971).
[28] S. P. Andreev, B. M. Karnakov, and V. D. Mur, Teor. Mat. Fiz. **64**, 287 (1985); Theor. Math. Phys. **64**, 838 (1985).
[29] S. P. Andreev, B. M. Karnakov, and V. D. Mur, Pis'ma Zh. Eksp. Teor. Fiz. **37**, 155 (1983) [JETP Lett. **37**, 187 (1983)].
[30] N. L. Manakov, M. V. Frolov, B. Borca, and A. F. Starace, J. Phys. B **36**, R49 (2003).
[31] M. V. Frolov, N. L. Manakov, E. A. Pronin, and A. F. Starace, J. Phys. B **36**, L419 (2003).

[32] L. V. Keldysh, Zh. Eksp. Teor. Fiz. **47**, 1945 (1964) [Sov. Phys. JETP **20**, 1307 (1965)].
[33] M. V. Frolov, A. V. Flegel, N. L. Manakov, and A. F. Starace, Phys. Rev. A **75**, 063407 (2007).
[34] M. V. Frolov, A. V. Flegel, N. L. Manakov, and A. F. Starace, Phys. Rev. A **75**, 063408 (2007).
[35] M. V. Frolov, N. L. Manakov, and A. F. Starace, Phys. Rev. A **79**, 033406 (2009).
[36] M. Lewenstein, Ph. Balcou, M. Yu. Ivanov, A. L'Huillier, and P. B. Corkum, Phys. Rev. A **49**, 2117 (1994).
[37] M. V. Frolov, N. L. Manakov, A. A. Silaev, and N. V. Vvedenskii, Phys. Rev. A **81**, 063407 (2010).